Supplementary Information (SI) for Nanoscale.

α-Graphyne with Ultra-low Diffusion Barriers as a Promising Sodium-ion Battery Anode and a Computational Scheme for accurate estimation of Theoretical Specific Capacity

Babuji Dandigunta[†§‡], Abhijitha V G[†§], Sharma S.R.K.C. Yamijala[‡§], B.R.K. Nanda[†§*]

† Condensed Matter Theory and Computational Lab, Department of Physics,

Indian Institute of Technology Madras, Chennai-600036, India

‡ Computational Chemistry and Materials Science lab, Department of Chemistry, Indian Institute of Technology Madras, Chennai-600036, India.

§ Centre for Atomistic Modelling and Materials Design, Indian Institute of Technology Madras, Chennai-600036, India.

E-mail: nandab@iitm.ac.in

Table S1. Bader charge and adsorption energies at all possible adsorption sites of AGY 2×2 supercell.

Adsorption site (Fig. S1)	E_{ads} (eV)	Distance from AGY plane (nm)	Bader charge on Na
1	-0.284	0.242	+0.927
2	-0.299	0.247	+0.927
3	-0.901	0	+0.922
4	-0.899	0	+0.923
5	-0.903	0	+0.939

1. Possible adsorption configurations on 2×2 supercell of AGY

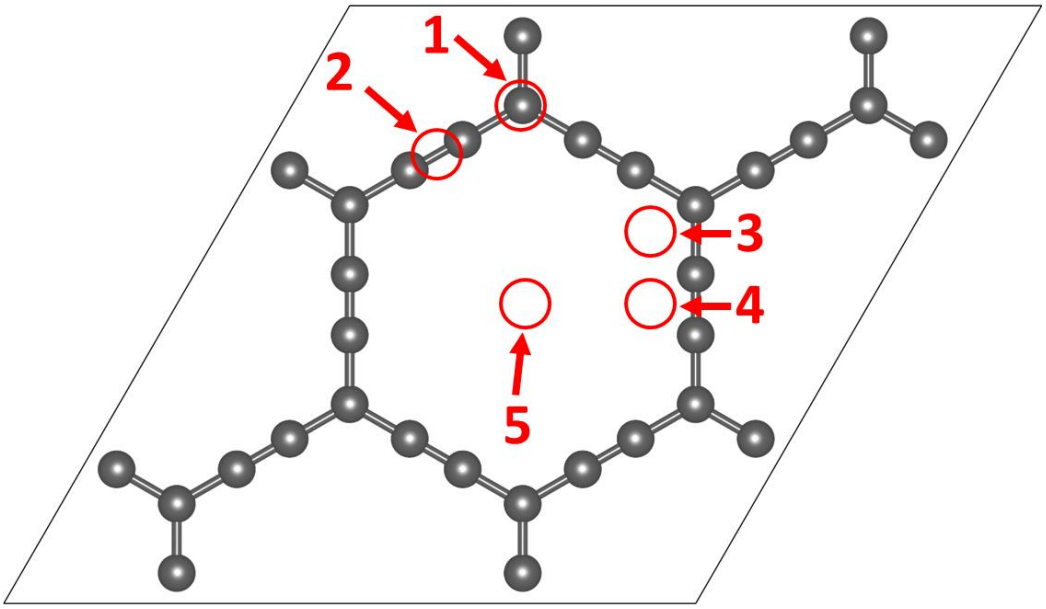

Figure S1. Adsorption sites were considered on 2×2 supercell of AGY in this study. Sites 2 and 5 are represented as sites I and II, respectively, in Fig. 1 (b,c) in the manuscript.

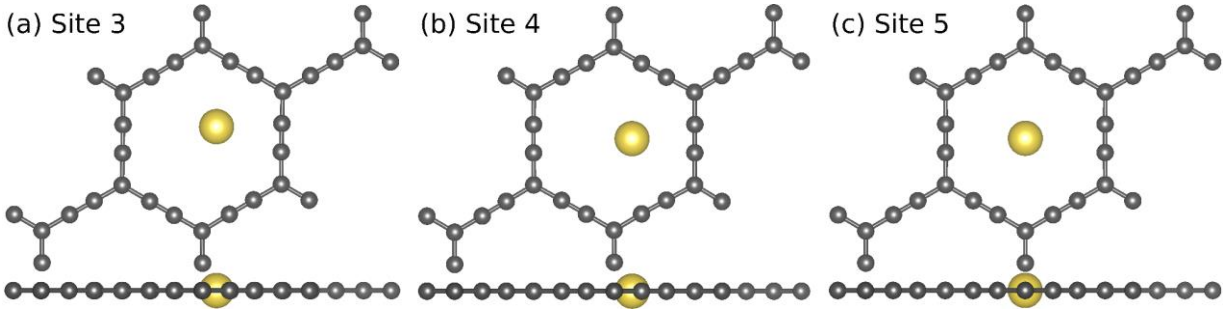

Figure S2. Final positions for (a) site 3 (b) site 4, and (c) site 5

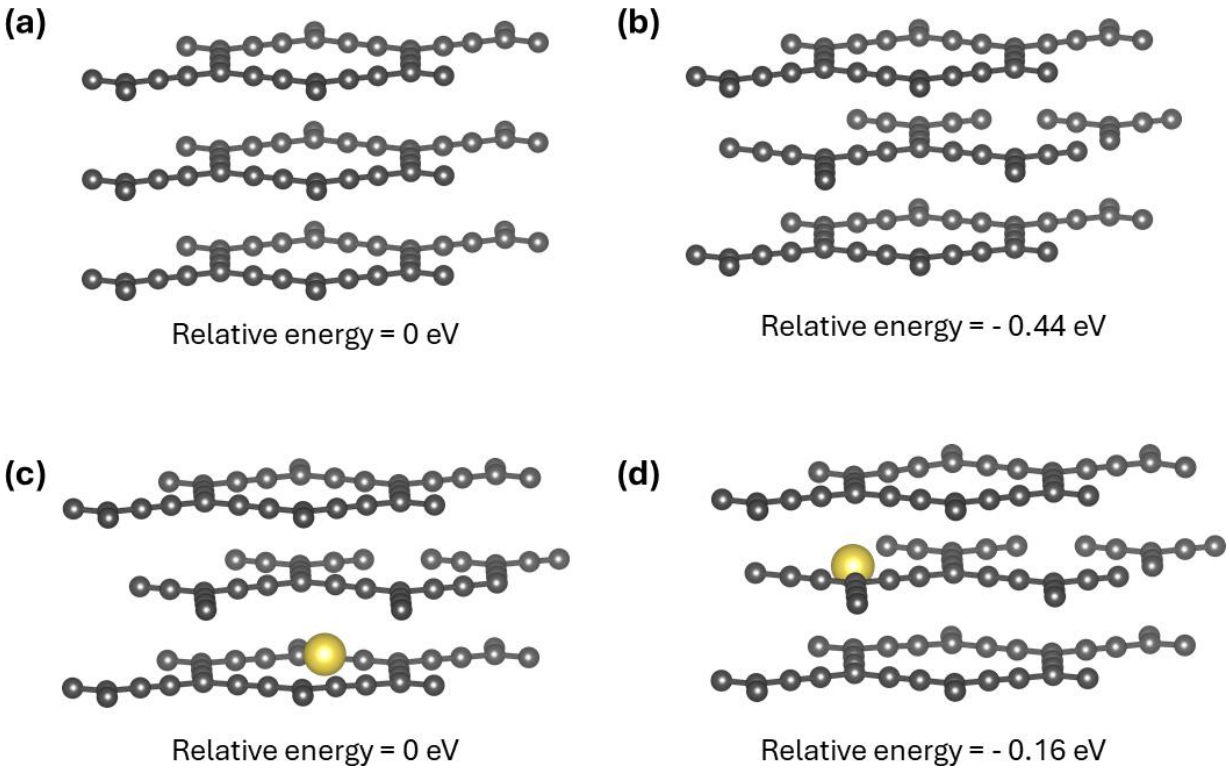

Figure S3. Relative energies of (a) AAA stacked, (b) ABA stacked AGY trilayer (relative energy is presented with respect to AAA-stacking). (c, d) Relative energies of Na adsorbed ABA-stacked AGY.

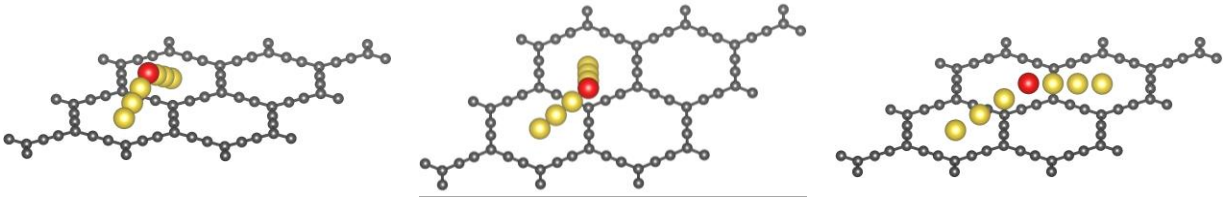

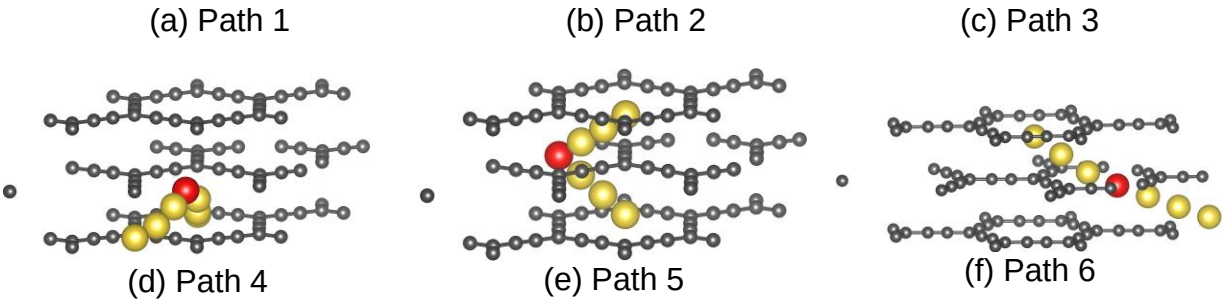

Figure S4. NEB images for diffusion paths of Na atom on monolayer and trilayer AGY. The red-colored atom in each image represents the intermediate reaction coordinate considered for the migration path.

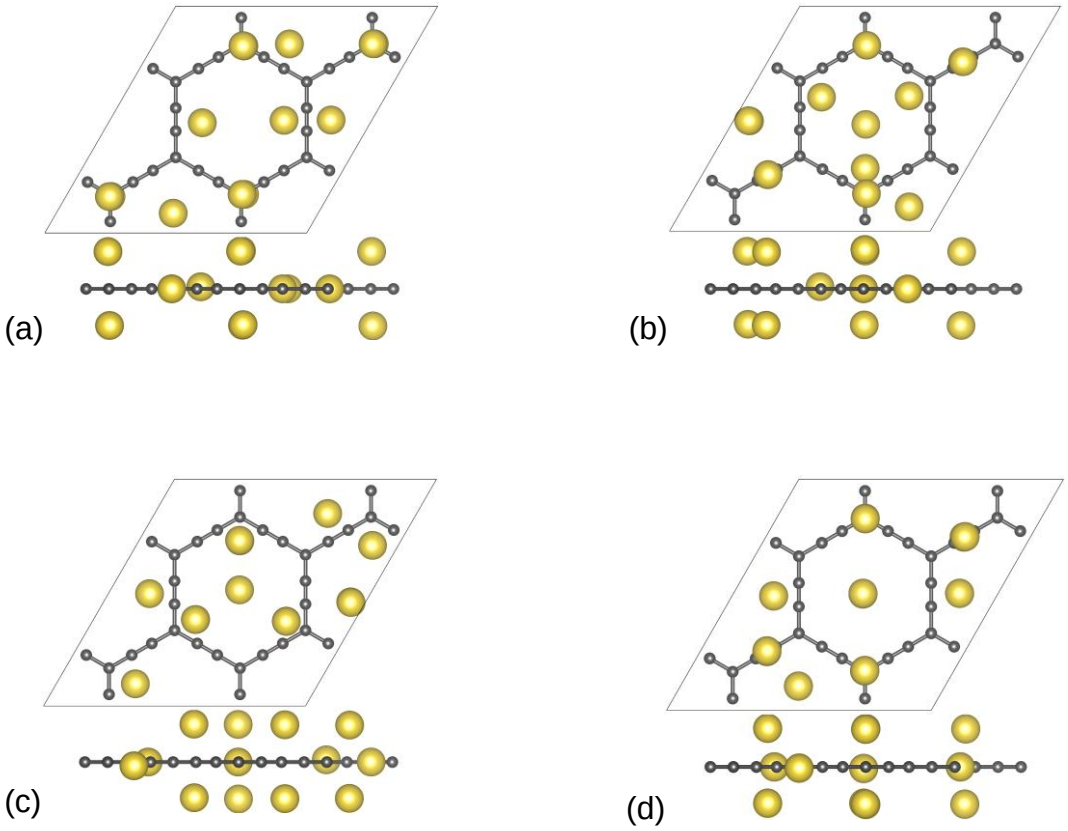

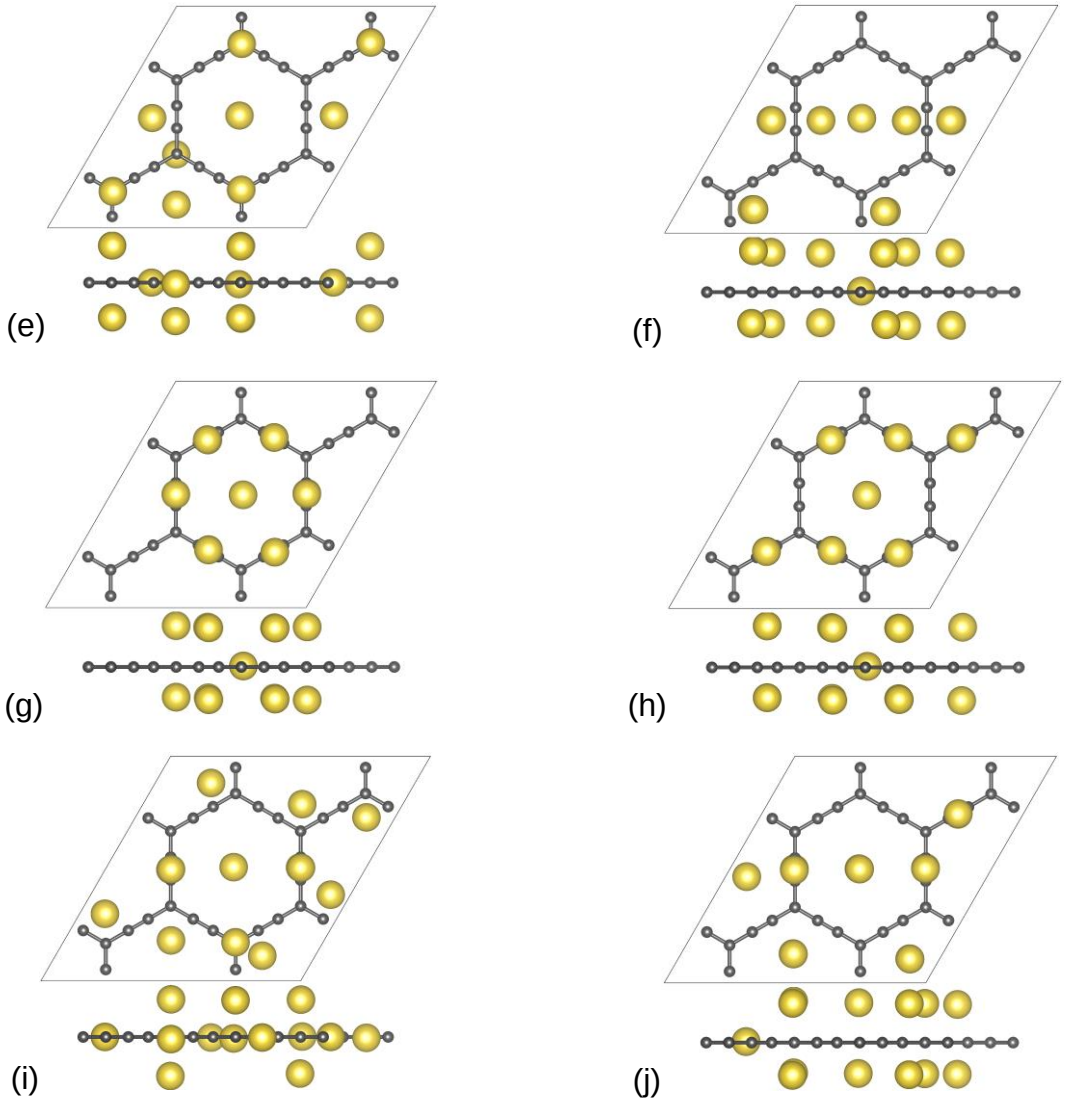

Figure S5. (a-i) Distinct initial configurations for loading 13 Na atoms on AGY.

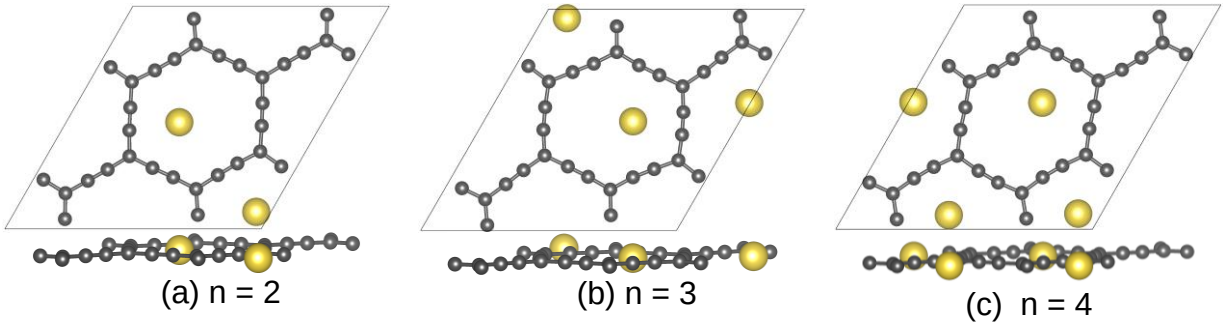

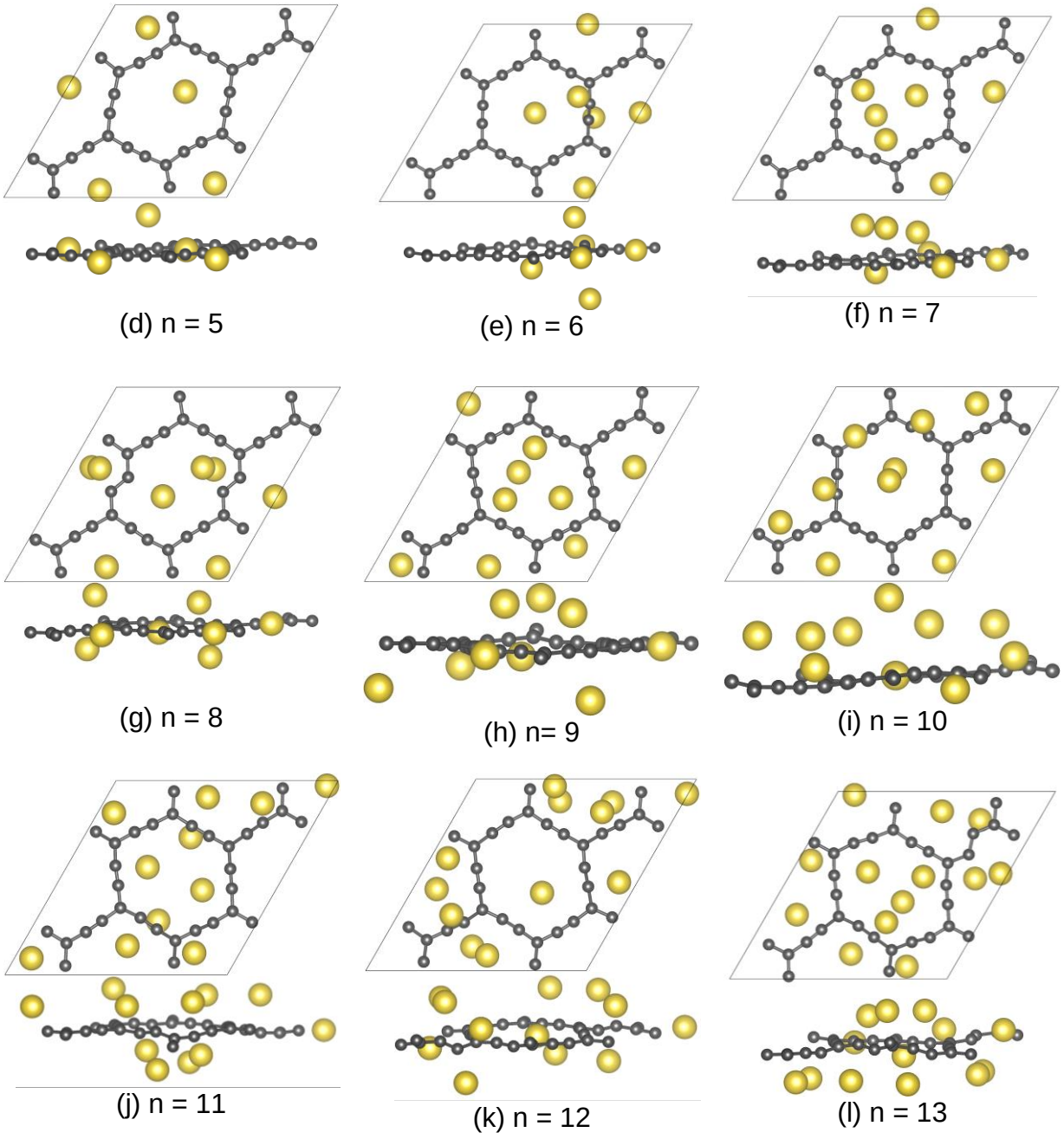

Figure S6. (a-l) Optimised geometries of hand-picked structural conformations of AGY 2×2 supercell loaded with n number of Na atoms.

(a1) (a2) (a3)

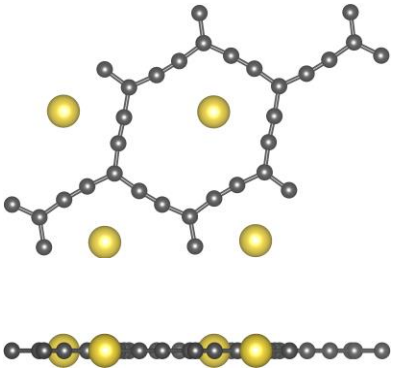

(a4)

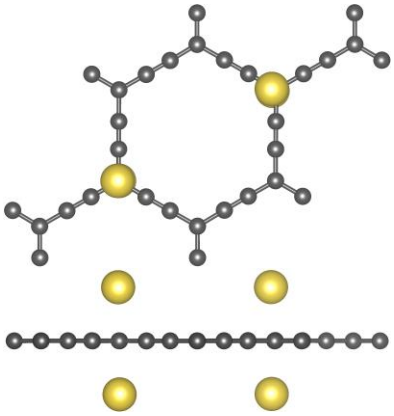

(a5)

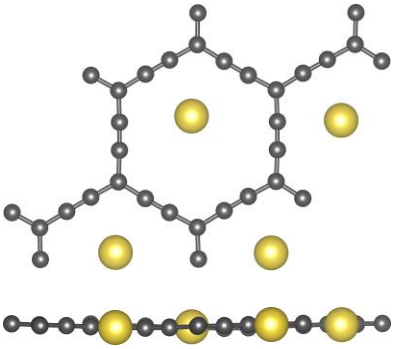

(a6)

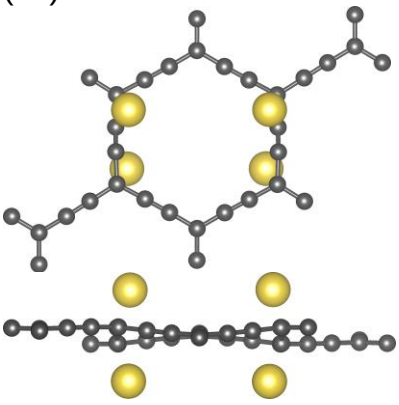

(a7)

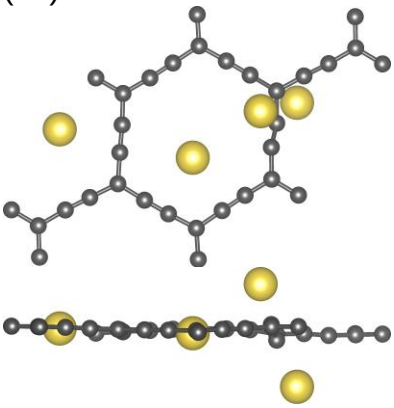

(a8)

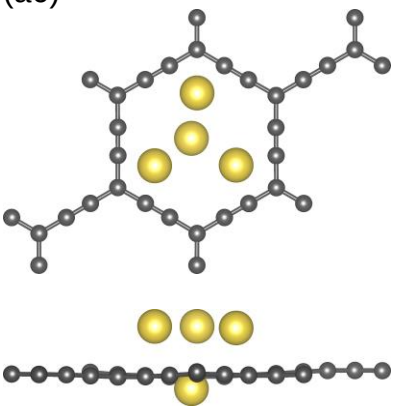

(a9)

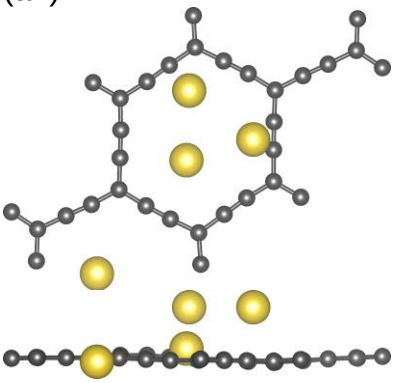

(a10)

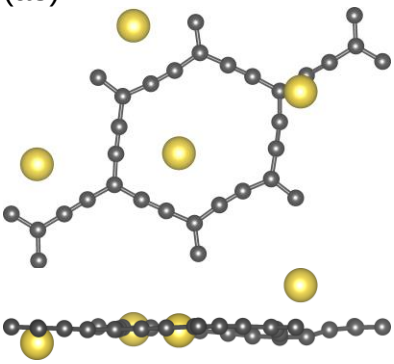

(b1)

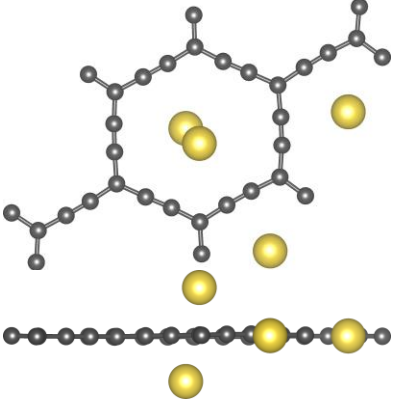

(b2)

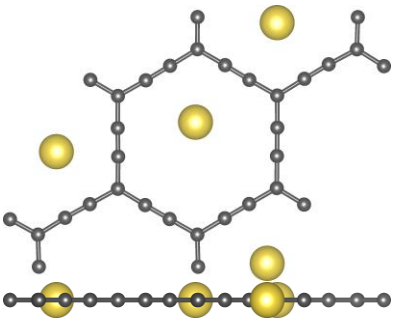

(b3)

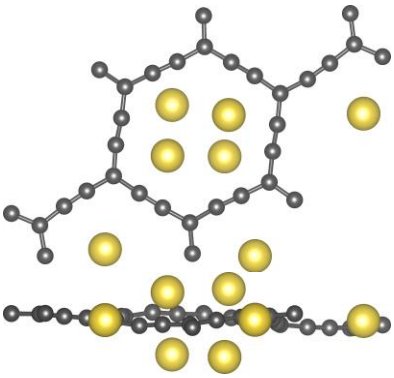

(b4)

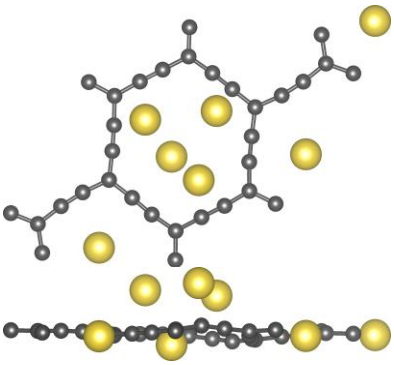

(b5)

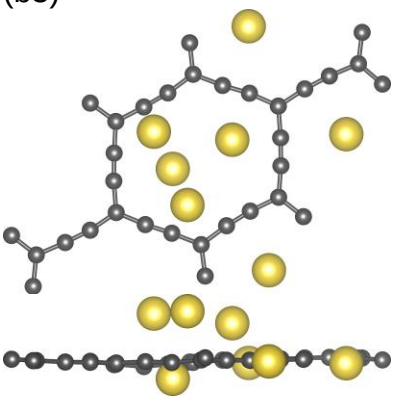

(b6)

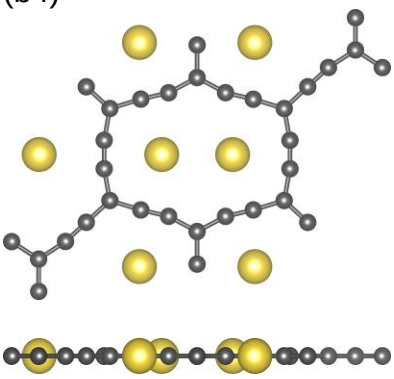

(b7)

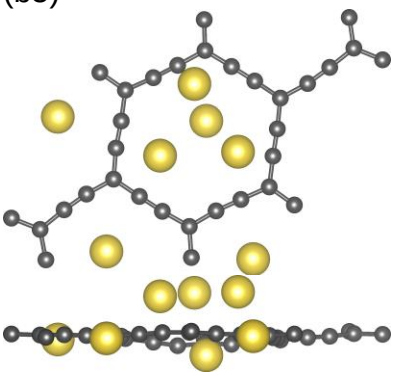

(b8)

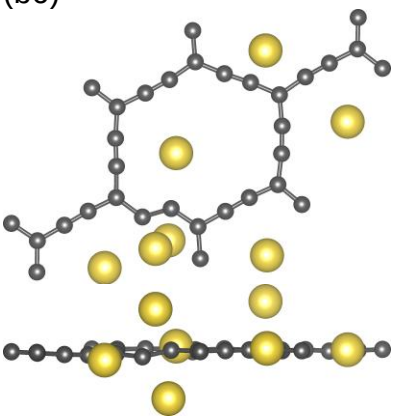

(b9)

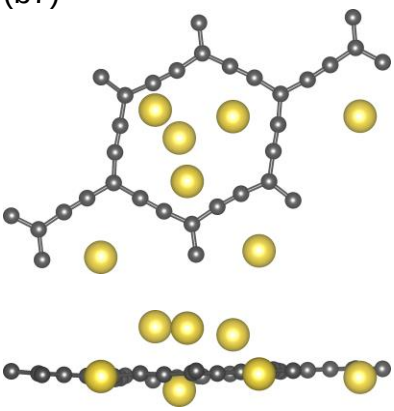

(b10)

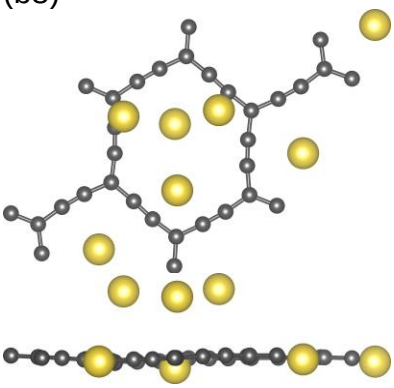

(c1)

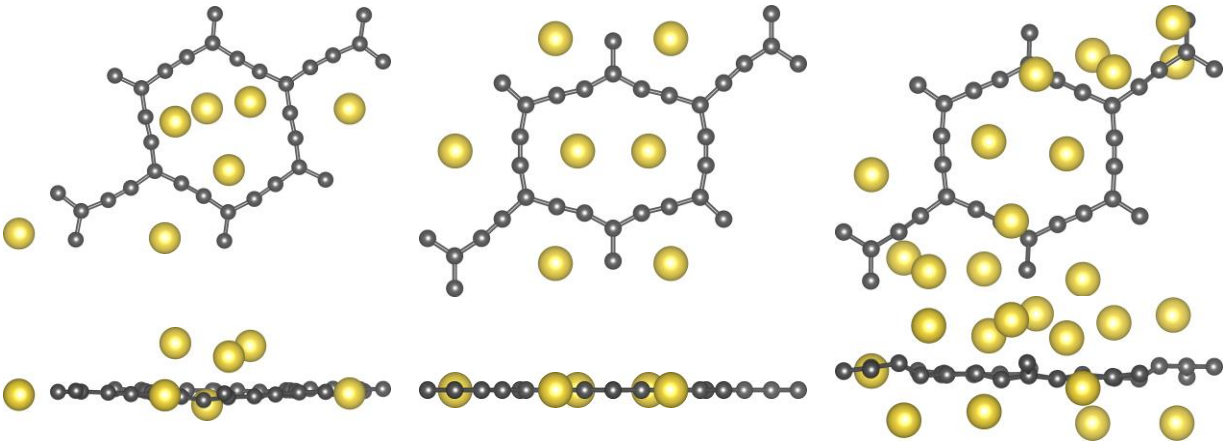

(c2)

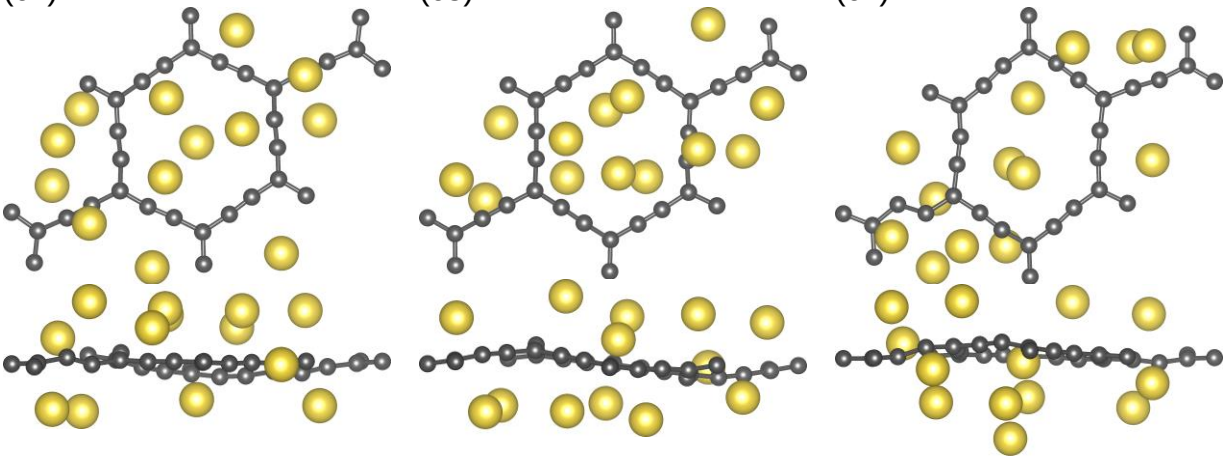

(c3)

(c4)

(c5)

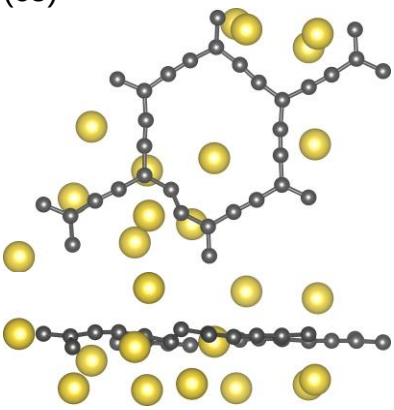

(c6)

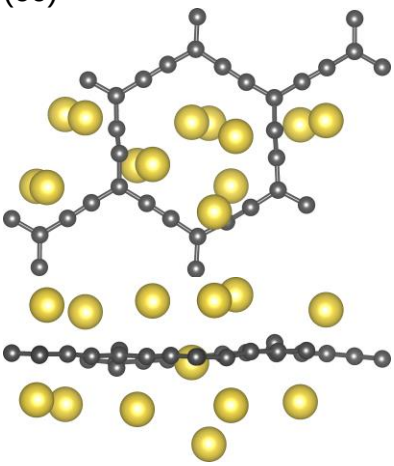

(c7)

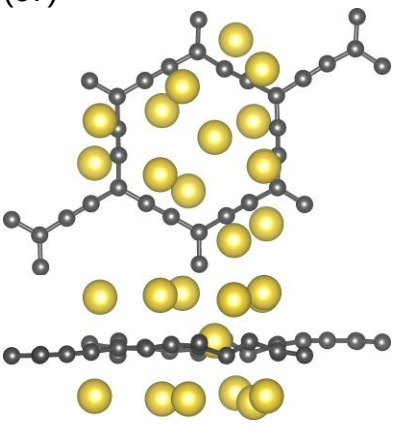

(c8)

(c9)

(c10)

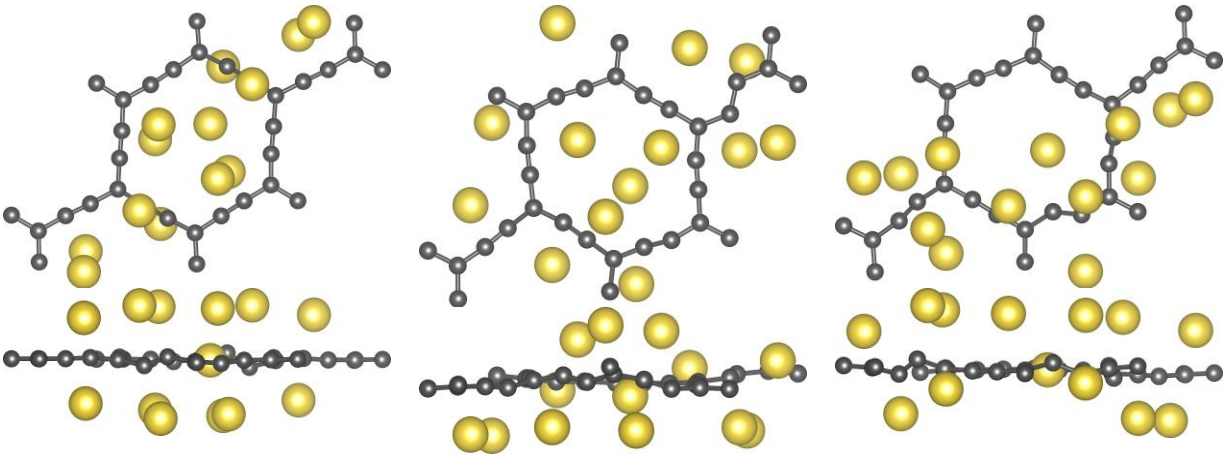

Figure S7. Final structures of the different input structures in the convex-hull-like approach for the same value of n in Na_nC_{32}, for (a1-a10) n = 4 (b1-b10) n = 7, and (c1-c10) n = 13.

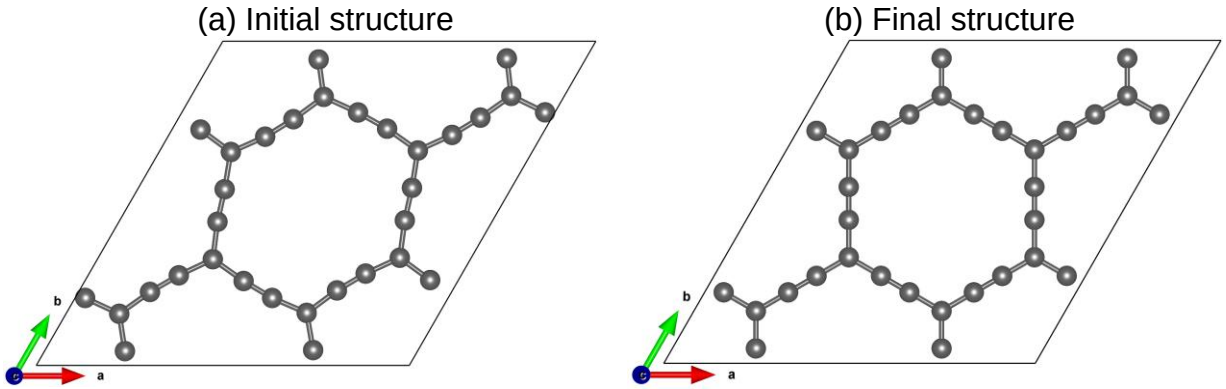

Figure S8. Cyclic durability study (a) Initial and (b) final structures of deformed α-graphyne. The structure obtained at the end of the AIMD simulation with four Na loading is selected and then we removed the loaded Na atoms, considering this structure as our initial configuration. Then we relaxed the structure and it reverted back to its pristine structure without any buckling, indicating its structural reversibility upon de/intercalation.

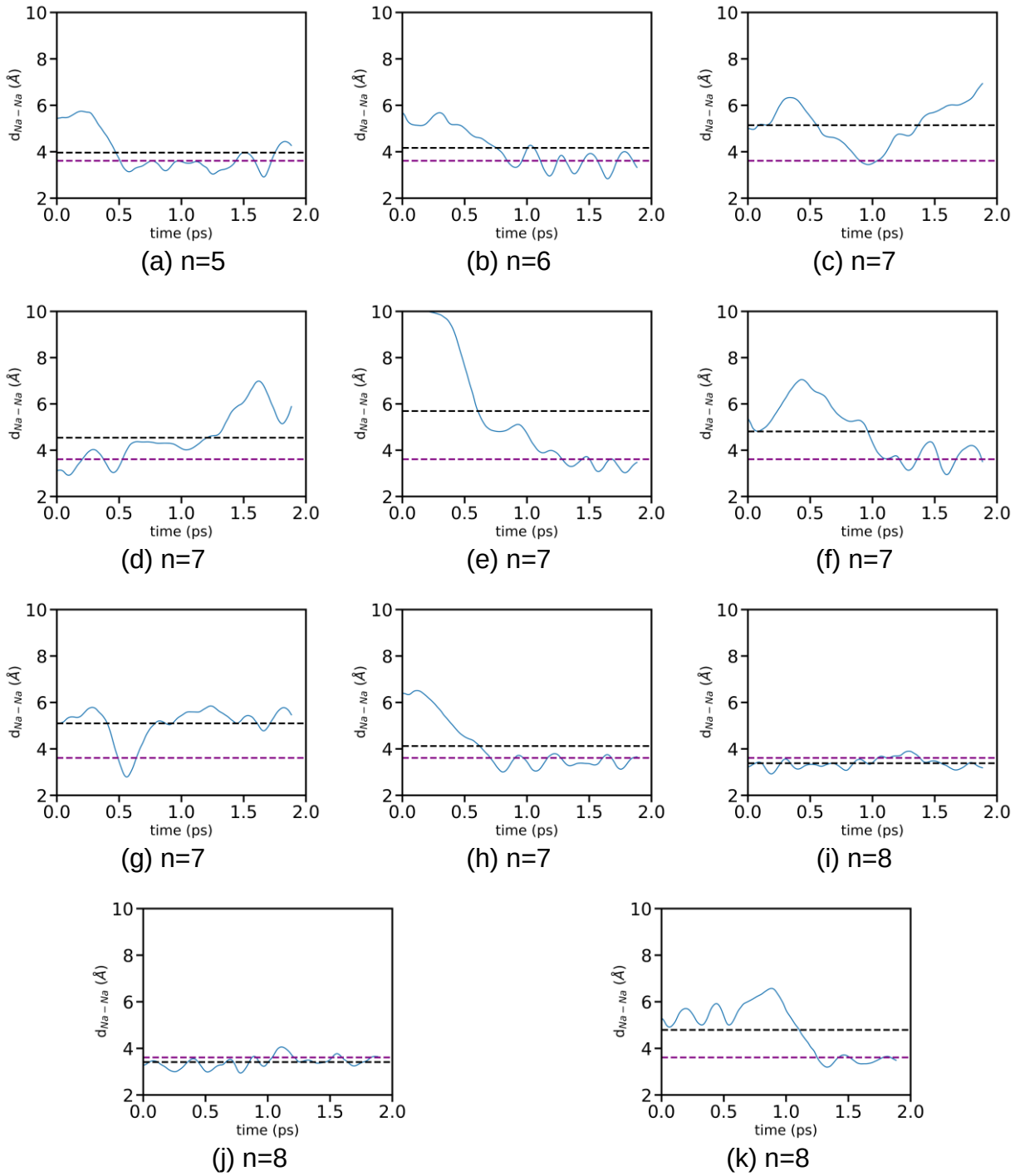

Figure S9. $d_{Na\text{-}Na}$ distance for each pair of Na atoms for a given value of 'n' where clustering is observed. (a) n=5 (b) n=6 (c-h) n=7 (i-k) n=8. At (i), strict clustering is observed where $d_{Na\text{-}Na,\ mean}$ (black dashed line) < $d_{Na\text{-}Na,\ Ref}$ (purple dashed line) for almost all the time.

S1. Structural and thermodynamical stability of doped AGY

Though B/N-doped AGY is yet to be experimentally synthesized, doping B and N atoms onto carbon allotropes is well-explored in the literature[1-6]. The B/N-doped graphdiyne and graphene structures are experimentally available[7, 8]. Furthermore, a previous theoretical study by Ruiz *et al.*[9] showed that B/N-doped AGY is geometrically and mechanically stable.

Table S2: Formation energies of different doping configurations in AGY.

Doping configuration	$E_{Formation}$ (eV)
B-sp^2	-0.32
B-sp	0.9
N-sp^2	1.4
N-sp	-0.26

Table S3: Cohesive energies of different doping configurations in AGY.

Doping configuration	$E_{Cohesive}$ (eV/atom)
B-sp^2	-8.147
N-sp	-8.191

The formation energy reported in Table S2 is defined as follows.

$$E_{Formation} = E_{products} - E_{reactants}$$

$$= (E_{B/N\text{-doped AGY}} + E_{C\ atom}) - (E_{pristine\ AGY} + E_{B/N\ atom})$$

The atomic energies are obtained from the cohesive energies of C, B, and N from their stable structural forms, viz., graphite, bulk boron, and N_2, respectively. We have

performed an AIMD calculation for the B/N-doped AGY at 700K to see the thermodynamical stability of the system.

- After a full structural relaxation of B/N-doped AGY, we found the force on the doped atom and the atoms in its neighbourhood is less than 0.001 eV/Å, implying that the doped structures are in a bound state and have a stable equilibrium.
- In addition, We have performed AIMD calculations for the B/N-doped AGY at 700K for 5ps to examine the thermodynamical stability of the system. As shown in Fig. S10(b, e), both B-doped AGY and N-doped AGY are thermodynamically stable even at high temperatures of 700K.
- N-doped AGY is more stable than B-doped AGY in terms of the formation energy data. Moreover, as shown in Fig. S10 (c, f), the bond lengths of B-C_{sp2}, N-C_{sp2}, and N-C_{sp} bonds are observed to have minimal fluctuations throughout the simulation, even at 700K.
- Moreover, we calculated the cohesive ($E_{Cohesive}$) and formation ($E_{Formation}$) energies. The values for the B (N) doped structures are $E_{Cohesive}$ = -8.147 eV/atom (-8.191 eV/atom) and $E_{Formation}$ = -0.32 eV (-0.26 eV). They are strong and negative, suggesting that they can be chemically synthesized.

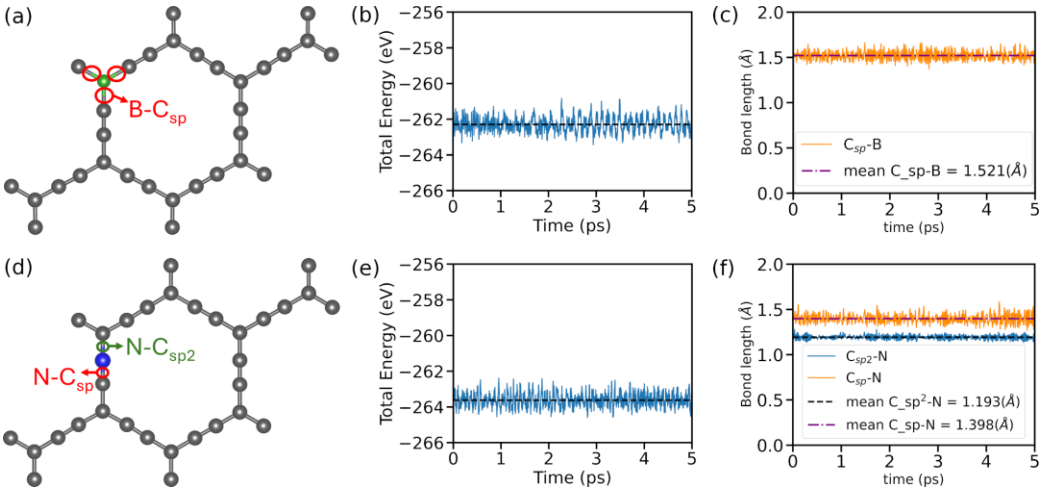

Figure. S10 Total energy of AGY doped with (a) boron (at sp^2 site), and (b) nitrogen atoms (at sp site), respectively at 700K.

S2. Two B/N atom doping on AGY

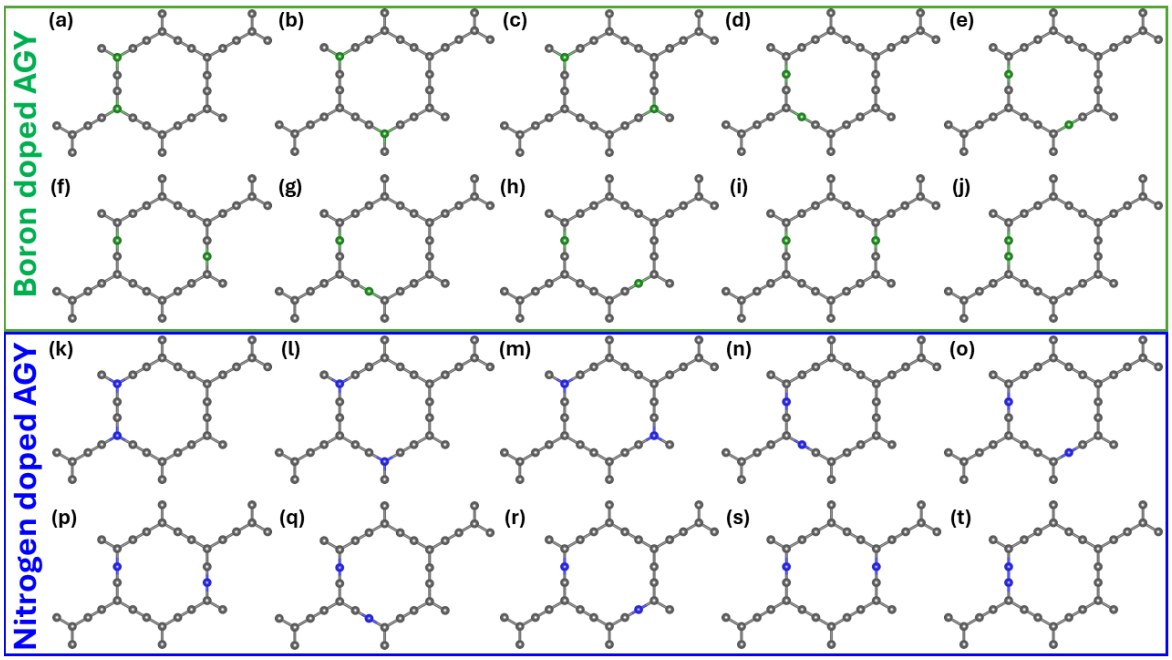

Figure S11. Optimised structures of dual atom doped AGY. (a-c) with two boron atoms at the sp^2 site, (d-j) with two boron atoms at the sp site. (k-m) Two nitrogen atoms at the sp^2 site, (n-t) two nitrogen atoms at the sp site

Table S4: Formation energies of dual atom doped AGY. (a-c) With two boron atoms at the sp^2 site, (d-j) with two boron atoms at the sp site. (k-m) Two nitrogen atoms at the sp^2 site, (n-t) two nitrogen atoms at the sp site

System	$E_{Formation}$ (eV)	System	$E_{Formation}$ (eV)	System	$E_{Formation}$ (eV)	System	$E_{Formation}$ (eV)
S11(a)	-0.53	S11(f)	1.65	S11(k)	2.73	S11(p)	-0.58
S11(b)	-0.45	S11(g)	1.90	S11(l)	2.88	S11(q)	-0.28
S11(c)	-0.76	S11(h)	1.71	S11(m)	2.49	S11(r)	-0.49
S11(d)	1.80	S11(i)	1.86	S11(n)	-0.25	S11(s)	-0.51
S11(e)	1.85	S11(j)	1.64	S11(o)	-0.47	S11(t)	1.87

We increased the doping concentration by substituting another carbon atom at either sp or sp^2 site. Here, we have considered ten configurations each for doping the second N or B atom, covering all possible doping sites. The optimized structures of two N, B doped AGY systems are presented in Fig. S11. We computed the formation energy of the doped systems with respect to the pristine AGY. The formation energy values reveal that boron atoms doped at all possible sp^2 sites (see Fig. S11(a-c)) and nitrogen atoms

doped at most of the sp sites (see Fig. S11(n-s)) are found to be energetically feasible (see Table S4). All other doped configurations exhibit a positive formation energy (see Fig. S11(d-m) and Table S4)

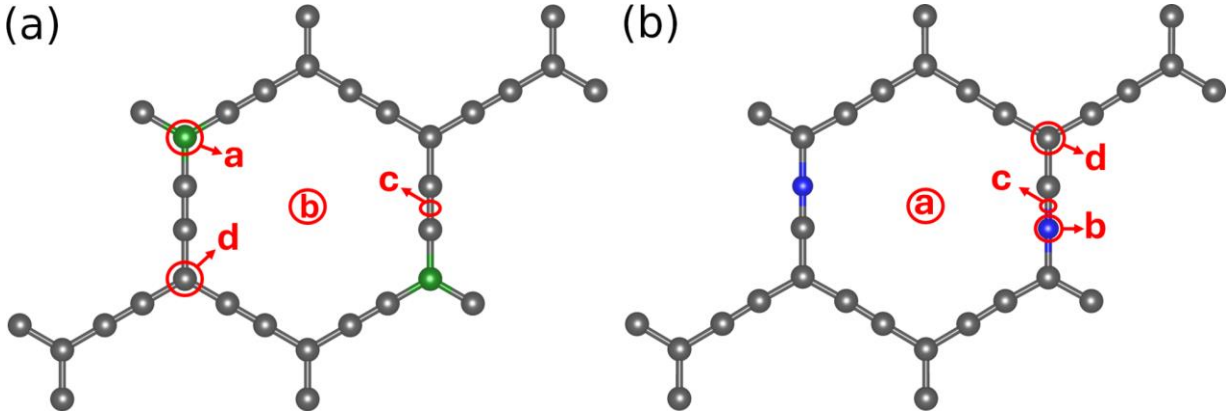

Figure S12. Sites considered for Na atom adsorption in dual atom doped AGY (here we have considered the configurations Fig. S11(c) boron-doped AGY, and Fig. S11(p) nitrogen-doped AGY for the adsorption study.

Table S5: Adsorption energy AGY doped with two B/N atoms.

AGY doped with two boron atoms		AGY doped with two nitrogen atoms	
Site	E_{ads} (eV)	Site	E_{ads} (eV)
a	-0.60	a	0.33
b	-0.95	b	0.71
c	-0.59	c	0.73
d	-0.43	d	-0.09

Interestingly, AGY doped with two nitrogen atoms is observed to be more stable than one nitrogen-doped AGY. The structures shown in Fig. S11(c) and Fig. S11(p) are observed to be most stable when the AGY is doped with two boron atoms and two nitrogen atoms, respectively, as mentioned in Table S4. We performed the Na adsorption study for these two structures by considering four adsorption sites each, as shown in Fig. S12. The results are shown in Table S5, and from the table, it is evident that the adsorption strength decreases in all the considered dual atom doped AGY

systems. To summarize, increasing the doping concentration of B/N atoms is not preferred to loading Na atoms to the AGY.

References

1. lyas Abduryim, Changcheng Chen, Linsong Gao, Shuangna Guo, Songya Wang, Ziyi Zhang, Yan Cai, Shuli Gao, Wen Chen, Xiaoning Guan, et al. Novel boron-doped biphenylene network as high-capacity anodes for metal ions batteries: From monolayer to bilayer structure. *The Journal of Physical Chemistry C*, 2024.
2. Xiaoqiong Ren, Ke Wang, Yue Yu, Daokun Zhang, Gang Zhang, and Yuan Cheng. Tuning the mechanical anisotropy of biphenylene by boron and nitrogen doping. *Computational Materials Science*, 222:112119, 2023.
3. Anukul K Thakur, Klaudia Kurtyka, Mandira Majumder, Xiaoqin Yang, Huy Q Ta, Alicja Bachmatiuk, Lijun Liu, Barbara Trzebicka, and Mark H Rummeli. Recent advances in boron- and nitrogen-doped carbon-based materials and their various applications. *Advanced materials interfaces*, 9(11):2101964, 2022.
4. LS Panchakarla, KS Subrahmanyam, SK Saha, Achutharao Govindaraj, HR Krishnamurthy, UV Waghmare, and CNR Rao. Synthesis, structure, and properties of boron-and nitrogen-doped graphene. *Advanced Materials*, 21(46):4726–4730, 2009.
5. Sumin Ha, Go Bong Choi, Seungki Hong, Doo Won Kim, and Yoong Ahm Kim. Substitutional boron doping of carbon materials. *Carbon letters*, 27:1–11, 2018.
6. Cantekin Kaykılarlı, Deniz Uzunsoy, Ebru Devrim S¸am Parmak, Mehmet Ferdi Fellah, and ¨Ozgen C¸olak C¸akır. Boron and nitrogen doping in graphene: an experimental and density functional theory (dft) study. *Nano Express*, 1(1):010027, 2020.
7. Yongjie Xu, Yong Yue, Fanan Kong, and Shijie Ren. Direct chemical synthesis of nitrogen-doped graphynes with high supercapacitance via a cross-coupling copolymerization strategy. *Chemical Engineering Journal*, 435:135121, 2022
8. Jingjie Wu, Marco-Tulio F Rodrigues, Robert Vajtai, and Pulickel M Ajayan. Tuning the electrochemical reactivity of boron-and nitrogen-substituted graphene. *Advanced Materials*, 28(29):6239–6246, 2016.

9. Antonio Ruiz-Puigdollers and Pablo Gamallo. DFT study of the role of n-and b-doping on structural, elastic and electronic properties of α-, β-and γ-graphyne. *Carbon*, 114:301–310, 2017.